



**HAL**  
open science

## Measurements of hydrogen cyanide (HCN) and acetylene (C<sub>2</sub>H<sub>2</sub>) from the Infrared Atmospheric Sounding Interferometer (IASI)

Valentin Duflot, D. Hurtmans, L. Clarisse, Y. R'Honi, C. Vigouroux, M. de Mazière, E. Mahieu, C. Servais, Cathy Clerbaux, Pierre-François Coheur

### ► To cite this version:

Valentin Duflot, D. Hurtmans, L. Clarisse, Y. R'Honi, C. Vigouroux, et al.. Measurements of hydrogen cyanide (HCN) and acetylene (C<sub>2</sub>H<sub>2</sub>) from the Infrared Atmospheric Sounding Interferometer (IASI). *Atmospheric Measurement Techniques*, 2013, 6 (4), pp.917-925. 10.5194/amt-6-917-2013 . hal-00742702

**HAL Id: hal-00742702**

**<https://hal.science/hal-00742702>**

Submitted on 16 Jun 2017

**HAL** is a multi-disciplinary open access archive for the deposit and dissemination of scientific research documents, whether they are published or not. The documents may come from teaching and research institutions in France or abroad, or from public or private research centers.

L'archive ouverte pluridisciplinaire **HAL**, est destinée au dépôt et à la diffusion de documents scientifiques de niveau recherche, publiés ou non, émanant des établissements d'enseignement et de recherche français ou étrangers, des laboratoires publics ou privés.



# Measurements of hydrogen cyanide (HCN) and acetylene (C<sub>2</sub>H<sub>2</sub>) from the Infrared Atmospheric Sounding Interferometer (IASI)

V. Dufлот<sup>1</sup>, D. Hurtmans<sup>1</sup>, L. Clarisse<sup>1</sup>, Y. R'honi<sup>1</sup>, C. Vigouroux<sup>2</sup>, M. De Mazière<sup>2</sup>, E. Mahieu<sup>3</sup>, C. Servais<sup>3</sup>, C. Clerbaux<sup>1,4</sup>, and P.-F. Coheur<sup>1</sup>

<sup>1</sup>Spectroscopie de l'Atmosphère, Service de Chimie Quantique et Photophysique, Université Libre de Bruxelles, 50 Av. F. D. Roosevelt, 1050, Brussels, Belgium

<sup>2</sup>Belgian Institute for Space Aeronomy (BIRA-IASB), 3, Av. Circulaire, 1180, Brussels, Belgium

<sup>3</sup>Institut d'Astrophysique et de Géophysique, Université de Liège, 17, Allée du 6 Août, 4000, Liège, Belgium

<sup>4</sup>Université Paris 06, Université Versailles-St. Quentin, CNRS/INSU, LATMOS-IPSL, Paris, France

Correspondence to: V. Dufлот (valentin.dufлот@ulb.ac.be)

Received: 5 October 2012 – Published in Atmos. Meas. Tech. Discuss.: 16 October 2012

Revised: 19 March 2013 – Accepted: 20 March 2013 – Published: 9 April 2013

**Abstract.** Hydrogen cyanide (HCN) and acetylene (C<sub>2</sub>H<sub>2</sub>) are ubiquitous atmospheric trace gases with medium lifetime, which are frequently used as indicators of combustion sources and as tracers for atmospheric transport and chemistry. Because of their weak infrared absorption, overlapped by the CO<sub>2</sub> Q branch near 720 cm<sup>-1</sup>, nadir sounders have up to now failed to measure these gases routinely. Taking into account CO<sub>2</sub> line mixing, we provide for the first time extensive measurements of HCN and C<sub>2</sub>H<sub>2</sub> total columns at Reunion Island (21° S, 55° E) and Jungfraujoch (46° N, 8° E) in 2009–2010 using observations from the Infrared Atmospheric Sounding Interferometer (IASI). A first order comparison with local ground-based Fourier transform infrared (FTIR) measurements has been carried out allowing tests of seasonal consistency which is reasonably captured, except for HCN at Jungfraujoch. The IASI data shows a greater tendency to high C<sub>2</sub>H<sub>2</sub> values. We also examine a nonspecific biomass burning plume over austral Africa and show that the emission ratios with respect to CO agree with previously reported values.

for HCN are attributed to biomass burning, other sources exist, including emissions by fossil fuel combustion and higher plants, bacteria and fungi. The primary sink of HCN is thought to be ocean uptake (Cicerone and Zellner, 1983; Li et al., 2000). However, the magnitudes of these sources and sinks remain uncertain (Li et al., 2009). For C<sub>2</sub>H<sub>2</sub>, Xiao et al. (2007) evaluated biofuel combustion to be the dominant source, followed by fossil fuel combustion and biomass burning. Reaction with hydroxyl radical (OH) is the main sink for C<sub>2</sub>H<sub>2</sub>, which may also act as a precursor of secondary organic aerosols (Volkamer et al., 2009).

Aside from their chemical properties, HCN and C<sub>2</sub>H<sub>2</sub> are useful tracers of atmospheric transport. Indeed, with a lifetime of 2–4 weeks (C<sub>2</sub>H<sub>2</sub>) (Logan et al., 1981) to 2–4 months (HCN) (Li et al., 2000), they are effective indicators of how the large-scale distribution of atmospheric pollutants is influenced by long-range transport of biomass and fossil fuel burning. Moreover, the study of the ratio C<sub>2</sub>H<sub>2</sub>/CO (carbon monoxide) can also help estimate the age of combustion plumes (Xiao et al., 2007).

There are only a limited number of long-term local measurements of HCN and C<sub>2</sub>H<sub>2</sub>, mainly from ground-based FTIR at selected stations of the Network for the Detection of Atmospheric Composition Change (NDACC, <http://www.ndacc.org>), even if C<sub>2</sub>H<sub>2</sub> is not a regular NDACC target species. Hence, strong uncertainties remain with regard to the magnitude of sources and sinks of HCN and C<sub>2</sub>H<sub>2</sub>, as well as to their spatial distribution and seasonality

## 1 Introduction

Biomass burning is a considerable source of atmospheric trace gases and aerosols at a global scale (Crutzen and Andreae, 1990). Examples include hydrogen cyanide (HCN) and acetylene (or ethyne, C<sub>2</sub>H<sub>2</sub>). While the primary sources

in the atmosphere (Li et al., 2009; Parker et al., 2011). Satellite sounders have provided considerable new information in the past years, with measurements from the Atmospheric Chemistry Experiment (ACE-FTS) (Lupu et al., 2009), the Michelson Interferometer for Passive Atmospheric Sounding (MIPAS) (Wiegele et al., 2012) and the Microwave Limb Sounder (MLS) (Pumphrey et al., 2011). These measurements were all made in limb geometry and consequently mostly in the upper troposphere or higher; also the spatial sampling from these instruments is limited. HCN and C<sub>2</sub>H<sub>2</sub> have recently been observed using the IASI infrared nadir-looking hyperspectral sounder in a specific biomass burning plume (Clarisse et al., 2011a), as well as in an anthropogenic pollution plume uplifted in the free troposphere (Clarisse et al., 2011b). The purpose of this paper is to show that HCN and C<sub>2</sub>H<sub>2</sub> columns can indeed be routinely retrieved from IASI spectra, even in absence of exceptional columns or uplift mechanisms. Having a twice daily global coverage and a 12 km diameter footprint at nadir, the IASI infrared sounder (Clerbaux et al., 2009) aboard the MetOp-A has an obvious potential for providing measurements of these two species globally, and with higher spatial resolution and temporal sampling than what has been obtained up to now. We describe time series and analyze the seasonality of the columns of these two species above two ground-based FTIR observation sites. We also look into the retrieval performances in a typical biomass burning plume.

## 2 Retrievals

HCN and C<sub>2</sub>H<sub>2</sub> are retrieved from IASI radiance spectra with an optimal estimation method (Rodgers, 2000) implemented in the radiative transfer model *Atmosphit* (Coeur et al., 2005), using absorption bands centered at 713 ( $\nu_2$ ) and 729 ( $\nu_5$ ) cm<sup>-1</sup>, respectively. Both bands are close to one *Q* branch of CO<sub>2</sub> centered near 720 cm<sup>-1</sup>, affected by line mixing and hence hampering the retrievals of HCN and C<sub>2</sub>H<sub>2</sub> when the CO<sub>2</sub> bands cannot be properly simulated. For instance, Clarisse et al. (2011a) had to remove the 715–725 cm<sup>-1</sup> spectral range from their fits for HCN and C<sub>2</sub>H<sub>2</sub> as their forward model did not take into account CO<sub>2</sub> line mixing.

The line mixing effect is due to the increasing overlap of *Q* lines with increasing pressure, which is such that the contributions of the various transitions are no more additive and the spectrum cannot be simulated by simply summing up the individual line profiles. This is explained theoretically by the fact that intermolecular collisions induce transfer of absorption intensity among the internal levels defining the optical transitions, thus resulting in intensity exchanges between the various spectral components (Hartmann et al., 2008).

The CO<sub>2</sub> line mixing effects are now taken into account in *Atmosphit* up to 30 km for a wide range of atmospheres (i.e. for a wide range of pressure-temperature profiles up to

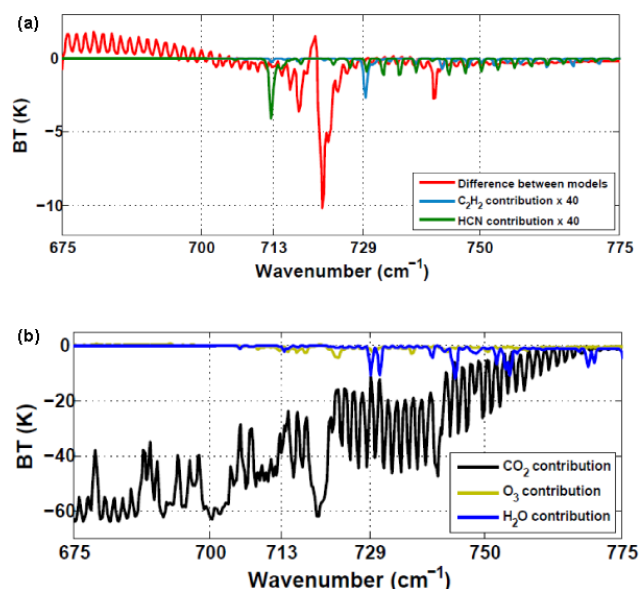


**Fig. 1.** (a) The red line shows the difference between the forward models with and without CO<sub>2</sub> line mixing considered. To make them visible, contributions of HCN (green line) and C<sub>2</sub>H<sub>2</sub> (blue line) are shown for background concentrations multiplied by 40. (b) Contribution of CO<sub>2</sub> (black line), O<sub>3</sub> (ochre line) and H<sub>2</sub>O (deep blue line) to a simulated spectrum for background concentrations in a standard atmosphere. Calculations have been made for the US Standard Atmosphere (US Government Printing Office, 1976) with CO<sub>2</sub> concentrations scaled to 390 ppmv.

30 km in order to cover all kind of atmospheres that can be encountered on earth) by calculating absorption cross sections of CO<sub>2</sub> following the method given in Gamache et al. (2012) and Lamouroux et al. (2012a, b). From 30 km to the top of the atmosphere, where collisions are less frequent, the individual line parameters from the HITRAN spectroscopic database (Rothman et al., 2009) are used. These are also used for all the other species in the line-by-line radiative transfer model.

Figure 1a (red line) shows the difference in the forward model between a spectrum simulated with and without line mixing, along with the spectral signature of HCN ( $\nu_2$ ) and C<sub>2</sub>H<sub>2</sub>( $\nu_5$ ) (green and blue lines, respectively). It is clear from the residual spectrum that the spectral fits of HCN and C<sub>2</sub>H<sub>2</sub> (and thus the retrievals of their abundance) are strongly dependent on the accuracy in the simulation of the CO<sub>2</sub> *Q* branch. For this study, line mixing is included throughout.

The inversion parameters detailed hereafter have been chosen to be the most general as possible. The purpose is to evaluate the capability of the retrieval strategy to detect HCN and C<sub>2</sub>H<sub>2</sub> routinely, without any specific assumptions on the vertical distribution of the target and interfering species. The retrievals are performed over the 675 to 775 cm<sup>-1</sup> spectral range and CO<sub>2</sub>, H<sub>2</sub>O and O<sub>3</sub> are fitted simultaneously as interfering species. Figure 1b shows the contributions of each

of these interfering species assuming background concentrations. For HCN and C<sub>2</sub>H<sub>2</sub>, we use an ad hoc covariance matrix with a 100 % variability and we assume the correlation from layer to layer being a 7 km-length exponential decay. These admittedly over simplistic assumptions allow stabilizing the retrieval without too much influence from the a priori information. The a priori profiles used for the forward model and the retrievals with *Atmosphit* are from the US standard atmospheres when spectra are analyzed over temperate latitudes, and from the standard tropical modeled atmosphere (Anderson et al., 1986) when spectra are analyzed over subtropical latitudes. HCN and C<sub>2</sub>H<sub>2</sub> are fitted as profiles, defined by 3 km thick layers from the ground up to 18 km, and by 7 km thick layers from 18 km up to 60 km. However, as the number of degrees of freedom for signal (DOFS) (Rodgers, 2000) is not larger than one for the two species, we analyze in the following only total columns.

### 3 Comparison with ground based FTIR measurements

We compare in this section HCN and C<sub>2</sub>H<sub>2</sub> total columns retrieved from IASI spectra and from ground-based FTIR spectra for the years 2009 and 2010 for two selected NDACC observation sites: Reunion Island (21° S, 55° E) and Jungfraujoch (46° N, 8° E). Note that for both sites and both target species ground-based retrievals are performed in a spectral range between 3250 and 3332 cm<sup>-1</sup>, which is outside the range covered by IASI. There, the main interfering species is H<sub>2</sub>O and the CO<sub>2</sub> line mixing effects are less critical and are not accounted for. Total errors for ground-based measurements at Reunion Island are 17 % for both species and total errors for HCN and C<sub>2</sub>H<sub>2</sub> ground-based measurements at Jungfraujoch are 5 and 7 %, respectively. Detailed description of ground-based FTIR data set, retrieval method and error budget can be found in Vigouroux et al. (2012) for Reunion Island and in Mahieu et al. (2008) and Li et al. (2009) for Jungfraujoch. Abundances retrieved from IASI spectra are calculated as columns above the altitude of the stations: 50 m and 3580 m a.m.s.l. (above mean sea level) for Reunion Island and Jungfraujoch, respectively. IASI cloudy spectra were removed from the data set using a 10 % contamination threshold on the cloud fraction in the pixel, and a posterior filter was also applied to remove poor fits, corresponding to a residual root mean square (RMS) greater than  $4 \times 10^{-6}$  Wm<sup>-2</sup> msr<sup>-1</sup>. In all, 31 % of the total clear sky spectra fits were removed because of a high RMS fit error. The resulting mean total retrieval errors on the total columns for HCN and C<sub>2</sub>H<sub>2</sub> are 53 and 47 % at Reunion Island, and 92 and 77 % at Jungfraujoch. The random (including smoothing) and systematic errors were taken into account. The smoothing error was found to be the most significant for HCN at Reunion Island and for C<sub>2</sub>H<sub>2</sub> at Jungfraujoch (32 and 54 %, respectively), and the systematic error

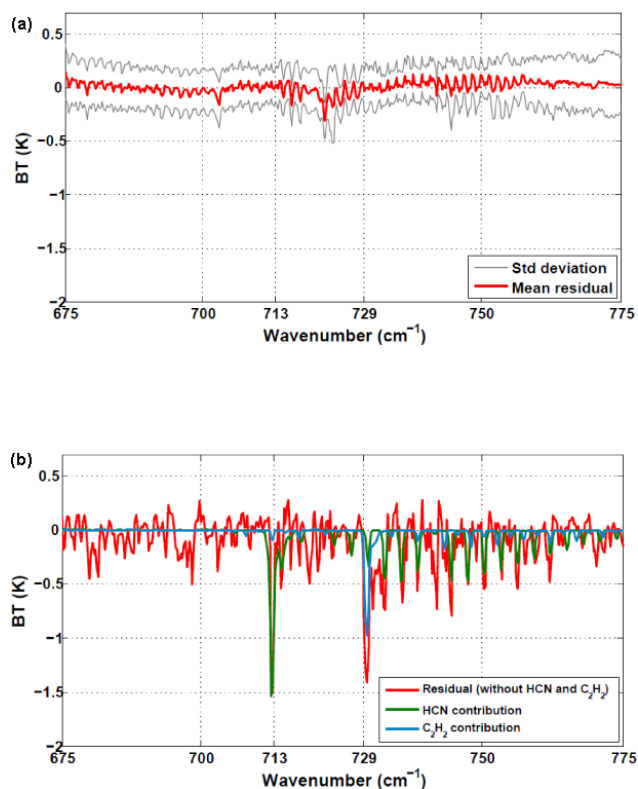


**Fig. 2.** (a) Residual averaged over the whole set of fits (red line) with its standard deviation (gray lines). (b) Difference (red line) between an observed spectrum on 10 October 2010 at 22.35° S and 33.63° E and the corresponding fitted spectrum when HCN and C<sub>2</sub>H<sub>2</sub> have been excluded from the fit. The green and blue lines show the contributions at the top of the atmosphere of HCN and C<sub>2</sub>H<sub>2</sub>, respectively.

was found to be the major one for C<sub>2</sub>H<sub>2</sub> at Reunion Island and for HCN at Jungfraujoch (42 and 75 %, respectively).

Figure 2a shows the residual averaged over the whole set of fits with its standard deviation. One can see that there is no noticeable residual bias except at  $\sim 720$  cm<sup>-1</sup> where it reaches  $-0.3$  K, which is close in absolute value to the instrumental noise of 0.2 K in this spectral region (Clerbaux et al., 2009).

Figure 3 shows the mean total column averaging kernels for IASI and for the ground-based FTIR at each of these sites, as well as the a priori profiles used in the retrievals (Fig. 3d). We find that the retrieved profiles from IASI spectra are mostly sensitive to the target species abundance in the mid-upper troposphere, with total column averaging kernels peaking at  $\sim 9$  km for C<sub>2</sub>H<sub>2</sub> for both sites, at  $\sim 10$  km for HCN at Jungfraujoch and at  $\sim 14$  km for HCN at Reunion Island. We also find that the retrieved profiles from IASI spectra are more sensitive to HCN abundance at Reunion Island than at Jungfraujoch, while the sensitivity to C<sub>2</sub>H<sub>2</sub> abundance is quite similar at both sites. Note that both ground-based instruments have a good sensitivity to HCN

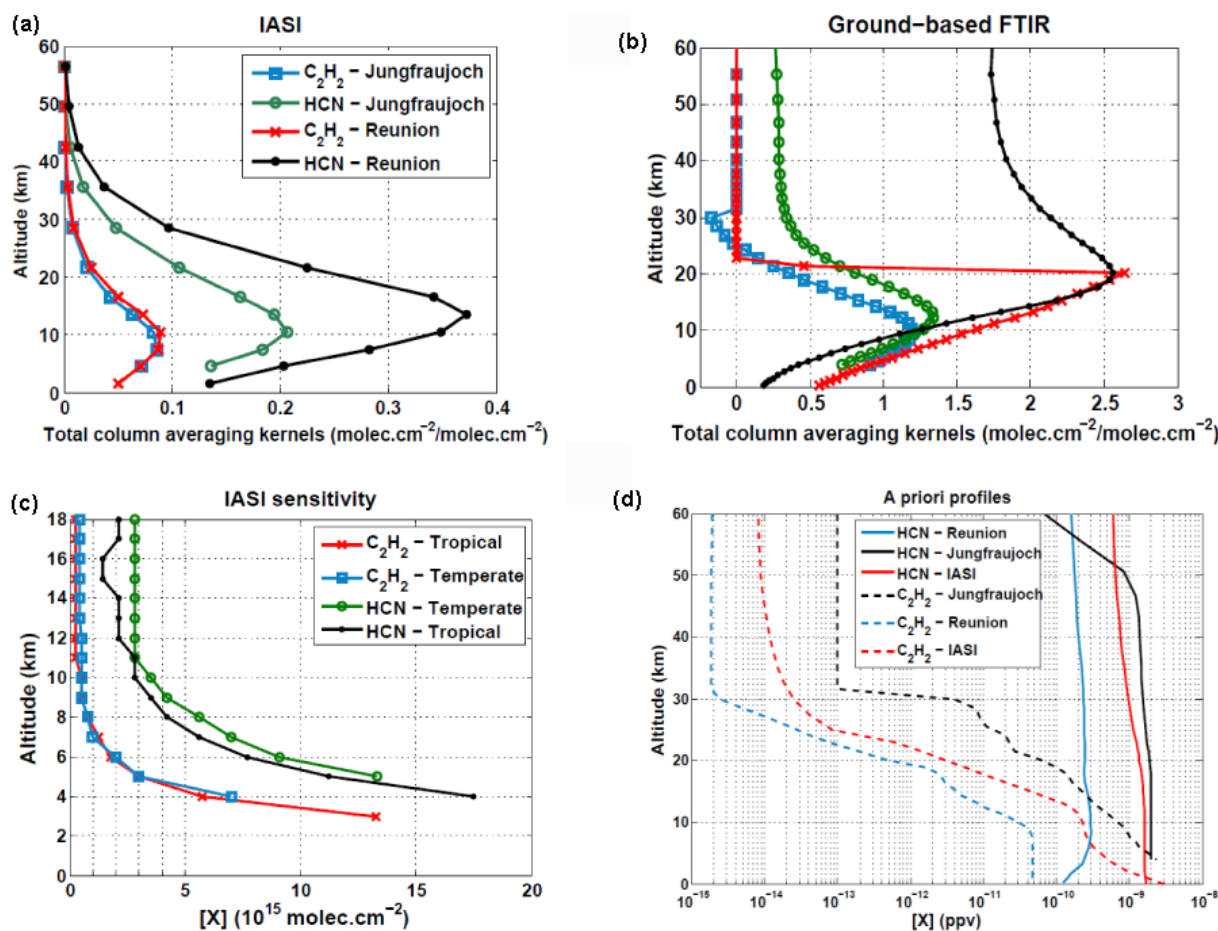


**Fig. 3.** (a) Total column averaging kernels of IASI and (b) ground-based FTIR in molecules cm<sup>-2</sup> for C<sub>2</sub>H<sub>2</sub> at Jungfrauoch (blue squares and lines), HCN at Jungfrauoch (green circles and lines), C<sub>2</sub>H<sub>2</sub> at Reunion and HCN at Reunion (black dots and lines). (c) Detectable concentrations by IASI as function of altitude for C<sub>2</sub>H<sub>2</sub> in a temperate atmosphere (blue squares and line), C<sub>2</sub>H<sub>2</sub> in a tropical atmosphere (red crosses and lines), HCN in a temperate atmosphere (green circles and lines) and HCN in a tropical atmosphere (black dots and line). (d) A priori profiles used in the retrievals for Reunion Island (blue lines), Jungfrauoch (black lines) and IASI (red lines) for HCN (solid lines) and C<sub>2</sub>H<sub>2</sub> (dotted lines).

abundance in the stratosphere, while IASI total column averaging kernels decrease rapidly to zero above the tropopause.

To further analyze the sensitivity of IASI to the target species, we simulated spectra with various HCN and C<sub>2</sub>H<sub>2</sub> concentrations for the standard temperate and tropical modeled atmospheres with CO<sub>2</sub> concentration scaled to a volume mixing ratio (vmr) of 390 ppmv. For this sensitivity analysis, HCN and C<sub>2</sub>H<sub>2</sub> profiles have been constructed, with enhanced concentrations of the species located in a 1 km thick layer, whose altitude is varied from the ground up to 18 km (mean maximal tropical tropopause height). The simulated spectra were compared one by one to a standard spectrum (i.e. with background concentrations of the trace gases) and if the difference between the two spectra was higher than the instrumental spectral noise in this region (0.2 K), then the enhanced concentration was tagged as detectable. Figure 3c summarizes the results. We find that IASI is able to detect

HCN (C<sub>2</sub>H<sub>2</sub>) concentrations lower than  $20 \times 10^{15}$  mol cm<sup>-2</sup> above 4 km (3 km) for a tropical atmosphere, and above 5 km (4 km) for a temperate atmosphere. For the tropical atmosphere, the maximum sensitivity is reached for HCN (C<sub>2</sub>H<sub>2</sub>) at 15 km (11 km) with a detectable concentration of  $1.4 \times 10^{15}$  ( $0.25 \times 10^{15}$ ) mol cm<sup>-2</sup>, while for the temperate atmosphere, the maximum sensitivity is reached for HCN (C<sub>2</sub>H<sub>2</sub>) at 11 km (13 km) with a detectable concentration of  $2.8 \times 10^{15}$  ( $0.4 \times 10^{15}$ ) mol cm<sup>-2</sup>.

Figure 4 shows the comparison between the IASI and the ground-based measurements. IASI retrieved total columns were averaged on a daily basis and on a 1° × 1° area around the observation sites. The comparison of the space and ground-based retrievals was performed taking into account the differences in the a priori profiles and in the sensitivity of the instruments. This has been done following the method given in Rodgers and Connor (2003): the retrieval sets have

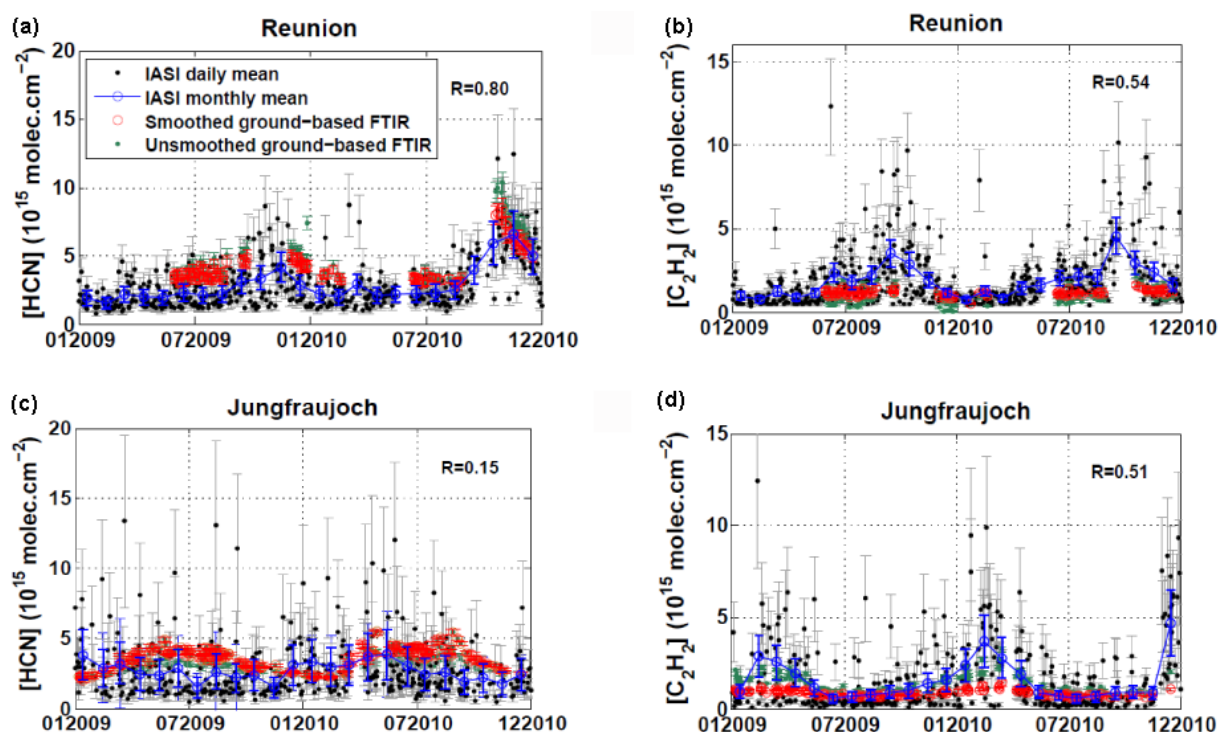


**Fig. 4.** Time series of HCN and C<sub>2</sub>H<sub>2</sub> measurements for Reunion Island (a and b) and Jungfraujoch (c and d). IASI measurements are shown as daily and 1° × 1° means (black dots) with associated total retrieval error (gray lines), and as monthly and 1° × 1° means (blue circles and line) with associated total retrieval error (vertical blue lines). Ground-based FTIR measurements smoothed (unsmoothed) with respect to IASI averaging kernels are shown as daily means with associated total error by red circles and line (green dots and line). Correlation coefficients of daily means are given on each plot: (a)  $R = 0.80$  (101 points), (b)  $R = 0.54$  (101 points), (c)  $R = 0.15$  (174 points), (d)  $R = 0.51$  (174 points).

been expressed in terms of departure from the comparison ensemble mean (to take into account the a priori profiles differences), and the ground-based measurements have been smoothed with respect to IASI averaging kernels (to take into account the sensitivity differences). Note that the similarity of the averaging kernel shapes (Fig. 3) for both instruments allows comparisons of total columns to be performed with some confidence. Red circles show ground-based measurements smoothed with respect to IASI averaging kernels, while green dots show unsmoothed ground-based measurements. Note that green dots are not visible when overplotted by red circles.

One can see that there is an overall agreement between the IASI and the ground-based FTIR measurements considering the error bars. An important result from this study is that IASI seems to capture the seasonality in the two species in most of the cases. This is best seen by looking at the IASI monthly mean retrieved total columns (blue circles and line in Fig. 4).

Note that the a priori total columns for ground-based measurements at Reunion Island are 4.9 and  $0.8 \times 10^{15}$  mol cm<sup>-2</sup> for HCN and C<sub>2</sub>H<sub>2</sub>, respectively, for ground-based measurements at Jungfraujoch they are 2.8 and  $1.3 \times 10^{15}$  mol cm<sup>-2</sup> for HCN and C<sub>2</sub>H<sub>2</sub>, respectively, and for IASI a priori to-

tal columns are 3.4 and  $1.2 \times 10^{15}$  mol cm<sup>-2</sup> for HCN and C<sub>2</sub>H<sub>2</sub>, respectively. The retrieved low values for each of the target species, sites and instruments being lower than the a priori total columns, these low values can be considered as significant. The scattering and discrepancies of the IASI daily mean measurements (black dots) are due to the averaging on a 1° × 1° area around the observation sites, and possibly to improvable fits (Fig. 2a).

At Reunion Island the HCN and C<sub>2</sub>H<sub>2</sub> peaks occur in October–November and are related to the Southern Hemisphere biomass burning season (Vigouroux et al., 2012). We find maxima of around  $5 \times 10^{15}$  molec cm<sup>-2</sup> for HCN and  $3 \times 10^{15}$  molec cm<sup>-2</sup> for C<sub>2</sub>H<sub>2</sub>, with somewhat larger values in 2010 in comparison to 2009. The seasonality and inter-annual variability matches very well that of the FTIR measurements for HCN (correlation coefficient of 0.80 for the entire daily mean data set) but with the IASI columns being biased low by  $1.72 \times 10^{15}$  molec cm<sup>-2</sup> when considering the smoothed ground-based measurements. The results are less satisfactory for C<sub>2</sub>H<sub>2</sub> (correlation coefficient of 0.54 for the entire daily mean data set) due to a high bias of  $0.67 \times 10^{15}$  molec cm<sup>-2</sup> for IASI. When considering unsmoothed ground-based measurements and error bars, the

magnitudes of the annual cycles for C<sub>2</sub>H<sub>2</sub> at Reunion Island captured by IASI and by ground-based FTIR are quite similar, except for two simultaneous measurements in September 2009. However, there is a lack of ground-based measurements during the biomass burning seasons (especially in October) to check the accordance between the IASI and ground-based measured amplitudes. Ground-based measurements performed in October 2004 and 2007 at Reunion Island show C<sub>2</sub>H<sub>2</sub> total columns values up to  $\sim 4.5 \times 10^{15}$  molec cm<sup>-2</sup> (Fig. 4 in Vigouroux et al., 2012), which agree with the IASI monthly mean measured columns in October 2009 and 2010. This gives some confidence in the monthly mean peak values observed by IASI. Comparison of additional simultaneous measurements during the biomass burning season is needed to further analyze this.

For the Jungfraujoch site, the agreement between IASI and the FTIR retrieved columns is acceptable for C<sub>2</sub>H<sub>2</sub> ( $R = 0.51$ ) and the seasonality is similar. The larger columns caused by the increased C<sub>2</sub>H<sub>2</sub> lifetime in winter (Zander et al., 1991) are indeed retrieved in February by both instruments. Similarly to the measurements at Reunion Island, we note an apparent tendency of the ground-based FTIR towards lower columns of C<sub>2</sub>H<sub>2</sub> than IASI in the season of peak values: we find a maximum of about  $3 \times 10^{15}$  molec cm<sup>-2</sup> for the IASI monthly mean and the unsmoothed ground-based measurements, and of about  $1.8 \times 10^{15}$  molec cm<sup>-2</sup> for the smoothed ground-based measurements. The most important disagreement is found for HCN at the Jungfraujoch site. The correlation coefficient is only 0.15 and the seasonality observed from the ground, showing higher values from spring to autumn due to northern African and boreal Asian biomass burning activity (Li et al., 2009), is not captured by IASI, which in fact does not seem to show any clear seasonal variation. This is likely to be due to the fact that in a temperate mid-latitude atmosphere, the IASI sensitivity to tropospheric HCN is lower than in a tropical atmosphere as shown in Fig. 3a and c. Moreover, stratospheric variations in HCN abundance, which are likely seen in the FTIR time series (Fig. 3b), are not captured by IASI.

To figure out the precision gained when including the CO<sub>2</sub> line mixing effects in the retrievals, we performed a set of retrievals without CO<sub>2</sub> line mixing on 500 randomly chosen spectra measured above the two sites. We found that including CO<sub>2</sub> line mixing effects in the retrievals decreases the residual of a factor three and increases the percentage of converging retrievals from 52 to 86 %. Moreover, note that if CO<sub>2</sub> line mixing effects are not considered in the IASI retrievals, retrieved total columns from IASI spectra do not agree any more with ground-based measurements: for both sites and both target species, IASI measurements become around one order of magnitude higher than the ground-based ones. This shows the importance of taking into account CO<sub>2</sub> line mixing effects in the forward and inverse models of the retrieval method when using absorption bands close to 720 cm<sup>-1</sup>.

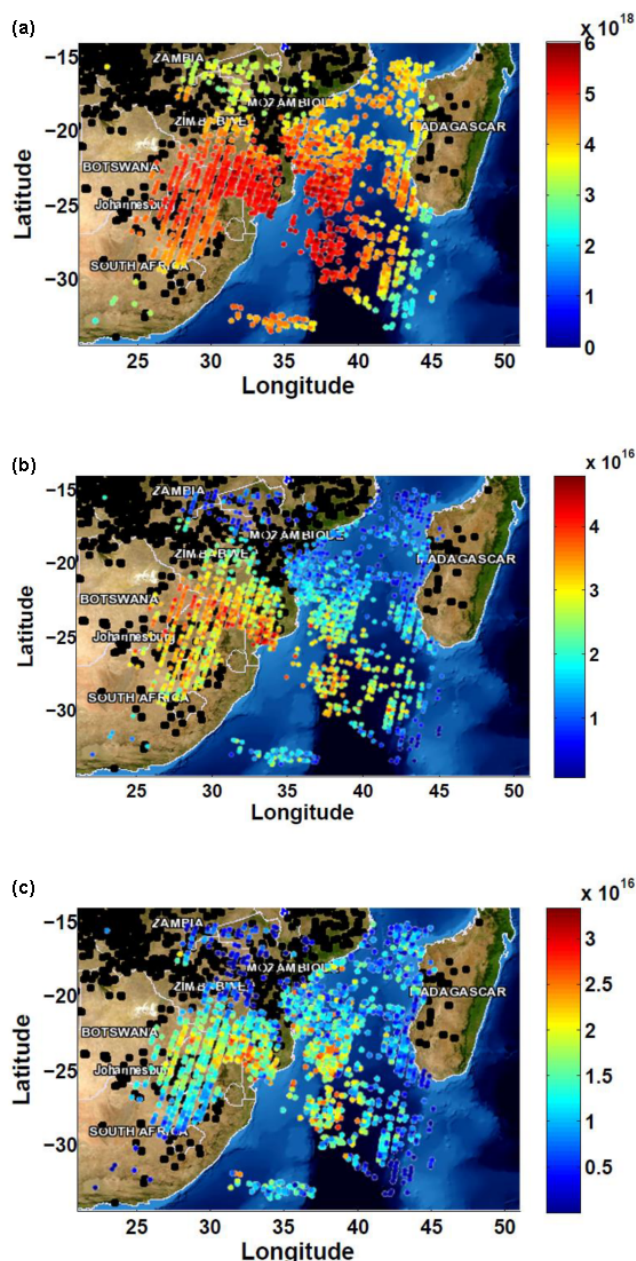
#### 4 Case study: an austral African biomass burning plume

To further illustrate what can be achieved with the measurements of HCN and C<sub>2</sub>H<sub>2</sub> total columns from IASI spectra, this section expounds the study of Clarisse et al. (2011a) for an exceptional fire event, to a regular biomass burning plume. We choose an event that took place over austral Africa and southern Mozambique Channel on 10 October 2010, which constitutes a typical biomass burning plume within the so-called “River of smoke” yearly exiting southern Africa toward the southern Indian Ocean during the Southern Hemisphere biomass burning season (Annegarn et al., 2002; Dufлот et al., 2010). To test the validity of the retrieval method for the widest range of situations, the retrievals were performed as exposed in Sect. 2, without any assumption on the altitude of the plume.

Figure 2b shows in red the difference between an observed spectrum on 10 October AM at 22.35° S and 33.63° E and the corresponding fitted spectrum with HCN and C<sub>2</sub>H<sub>2</sub> excluded. A number of absorption features (most notably at 713 and 729 cm<sup>-1</sup>) exceed the instrumental noise and can be attributed to HCN and C<sub>2</sub>H<sub>2</sub> when compared to the top of the atmosphere contribution of these species (shown in green and blue for HCN and C<sub>2</sub>H<sub>2</sub>, respectively). In fact, the maximum radiance difference reaches 1.5 K for HCN and C<sub>2</sub>H<sub>2</sub>, which is an order of magnitude larger than the instrumental noise of 0.2 K in this region (Clerbaux et al., 2009).

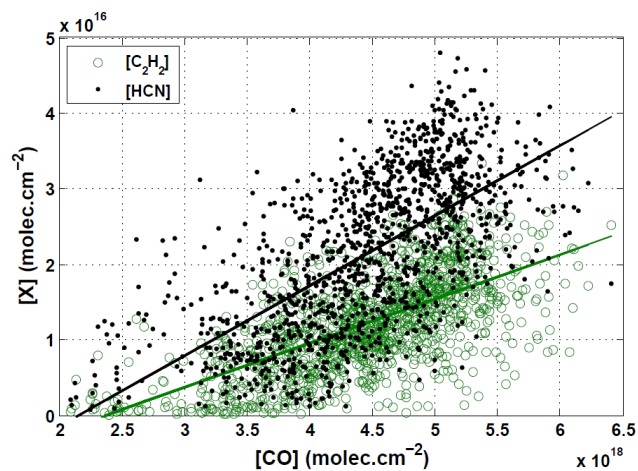
Figure 5 shows the total columns (in molecules cm<sup>-2</sup>) of CO (retrieved in near-real-time from FORLI software (Hurtmans et al., 2012)), HCN and C<sub>2</sub>H<sub>2</sub>, respectively, on 10 October. Note that to produce the distributions, the cloudy spectra were removed from the data set and retrievals with errors greater than 100 % were also excluded. The resulting mean total retrieval errors for HCN and C<sub>2</sub>H<sub>2</sub> total columns are 26 and 68 %. We see in Fig. 5 that the plume is similar in shape for the 3 species and extends from  $\sim (15^\circ \text{S}, 20^\circ \text{E})$  to  $\sim (35^\circ \text{S}, 45^\circ \text{E})$ . The biomass burning spots detected by the Moderate Resolution Imaging Spectroradiometer (MODIS) in Zambia, Mozambique, Zimbabwe, Botswana and South Africa on 9 and 10 October are shown by black dots in these figures. Due to the closeness of the fires and the typical seasonality of such an event, the detected plume originates very likely from those fires. Maximum columns in the plume reach  $5.9 \times 10^{18}$  for CO,  $4.8 \times 10^{16}$  for HCN and  $3.2 \times 10^{16}$  molecules cm<sup>-2</sup> for C<sub>2</sub>H<sub>2</sub>.

Figure 6 shows the correlation plot between CO and HCN (black dots) and C<sub>2</sub>H<sub>2</sub> (green circles) total columns. The correlation coefficients are 0.72 and 0.68 for HCN and C<sub>2</sub>H<sub>2</sub>, respectively, for a total of 1397 retrieval points. This high correlation between the three species, which share biomass burning as an important source, confirms the fire origin of the plume. Given the relatively long lifetimes of the species (several weeks to several months) and the vicinity of the fire sources, the slope of each correlation line gives the



**Fig. 5.** Total columns of CO (a), HCN (b) and C<sub>2</sub>H<sub>2</sub> (c) on 10 October 2010. Fires spots detected by MODIS on 9 and 10 October are shown by the black dots.

emission ratio of the corresponding species:  $0.0092 \pm 0.0016$  and  $0.0055 \pm 0.0034$  for HCN and C<sub>2</sub>H<sub>2</sub>, respectively. These values compare very well with the emission ratios with respect to CO derived by Sinha et al. (2003) from aircraft measurements over savanna fires in Southern Africa ( $0.0085 \pm 0.0029$  for HCN and  $0.0043 \pm 0.0013$  for C<sub>2</sub>H<sub>2</sub>).



**Fig. 6.** Correlation plot between CO total columns and HCN (black dots) and C<sub>2</sub>H<sub>2</sub> (green circles) total columns for the day and region shown on Fig. 5. The correlation coefficients are 0.72 (1397 points) and 0.68 (1397 points) for HCN and C<sub>2</sub>H<sub>2</sub>, respectively.

## 5 Conclusion and outlooks

We have demonstrated the possibility of retrieving HCN and C<sub>2</sub>H<sub>2</sub> columns from IASI radiance spectra in the  $720 \text{ cm}^{-1}$  region, by properly incorporating CO<sub>2</sub> line mixing in the radiative transfer model. This study shows that the sensitivity of IASI to the two species is mostly in the mid-upper troposphere above 6 km. Total columns have been retrieved for a two year period above Reunion Island and Jungfrau-joch, where routine FTIR measurements are available. The comparison between IASI and FTIR retrieved total columns demonstrates the capabilities of IASI to capture the seasonality in HCN and C<sub>2</sub>H<sub>2</sub> in most cases (HCN and to lesser extent C<sub>2</sub>H<sub>2</sub> at Reunion Island; and C<sub>2</sub>H<sub>2</sub> at Jungfrau-joch). We also note a greater tendency of IASI data to high C<sub>2</sub>H<sub>2</sub> values. The absence of seasonality of HCN at Jungfrau-joch could be rationalized by the low sensitivity of IASI to HCN abundance at mid-latitudes. The IASI total columns of HCN (C<sub>2</sub>H<sub>2</sub>) are shown in this preliminary comparison to be biased low (high) as compared to the smoothed ground-based measurements. A more complete validation study should be carried out to confirm this.

In addition, HCN and C<sub>2</sub>H<sub>2</sub> total columns were retrieved within a biomass burning plume over austral Africa and emission ratios with respect to CO were derived from these measurements. The values of  $0.0092 \pm 0.0016$  and  $0.0055 \pm 0.0034$  for HCN and C<sub>2</sub>H<sub>2</sub>, respectively, agree with values reported in the literature for biomass burning plumes above austral Africa.

In summary, the results presented in this paper have shown for the first time that IASI spectra can be used to establish time series and trends of HCN columns at tropical latitudes and C<sub>2</sub>H<sub>2</sub> columns at tropical and temperate latitudes, and both for background or highly concentrated (biomass



burning plume) environments. Due to a low sensitivity of IASI to HCN in a temperate atmosphere, this target specie cannot be considered as retrievable over mid-latitudes areas in background conditions. Work is ongoing to fully exploit the IASI spatial resolution and temporal sampling, to provide global distributions of these two species wherever its sensitivity to background conditions is sufficient.

*Acknowledgements.* IASI has been developed and built under the responsibility of the Centre National d'Etudes Spatiales (CNES, France). It is flown onboard the Met-Op satellites as part of the EUMETSAT Polar System. The IASI L1 data are received through the EUMETCast near real time data distribution service. Part of the research is supported by EUMETSAT through the O<sub>3</sub>SAF project. P. F. C. and L. C. are, respectively, Scientific Research Worker and Research Associate at the F.R.S.-FNRS. The research in Belgium was funded by the F.R.S.-FNRS, the Belgian State Federal Office for Scientific, Technical and Cultural Affairs and the European Space Agency (ESA Prodex arrangements C4000103226 and the AGACC-II project). Financial support by the "Actions de Recherche Concertées" (Communauté Française de Belgique) is also acknowledged. The Liège team further acknowledges the Fédération Wallonie-Bruxelles for supporting travel costs to the Jungfraujoch station and wishes to thank the International Foundation High Altitude Research Stations Jungfraujoch and Gornergrat (HFSJG, Bern) for supporting the facilities needed to perform the observations.

Edited by: H. Worden

## References

- Anderson, G. P., Clough, S. A., Kneizys, F. X., Chetwynd, J. H., and Shettle, E. P.: AFGL Atmospheric Constituent Profiles (0–120 km), Environmental Research Papers no. 954, Air Force Geophysics Laboratory, Hanscom AFB Massachusetts, AFGL-TR-86-0110, 1986.
- Annegarn, H. J., Otter, L., Swap, R. J., and Scholes, R. J.: Southern Africa's ecosystem in a test-tube: A perspective on the Southern African Regional Science Initiative (SAFARI 2000), *S. Afr. J. Sci.*, 98, 111–113, 2002.
- Cicerone, R. J. and Zellner, R.: The atmospheric chemistry of hydrogen cyanide (HCN), *J. Geophys. Res.*, 88, 10689–10696, 1983.
- Clarisse, L., R'Honi, Y., Coheur, P.-F., Hurtmans, D., and Clerbaux, C.: Thermal infrared nadir observations of 24 atmospheric gases, *Geophys. Res. Lett.*, 38, L10802, doi:10.1029/2011GL047271, 2011a.
- Clarisse, L., Fromm, M., Ngadi, Y., Emmons, L., Clerbaux, C., Hurtmans, D., and Coheur, P.-F.: Intercontinental transport of anthropogenic sulfur dioxide and other pollutants: An infrared remote sensing case study, *Geophys. Res. Lett.*, 38, L19806, doi:10.1029/2011GL048976, 2011b.
- Clerbaux, C., Boynard, A., Clarisse, L., George, M., Hadji-Lazaro, J., Herbin, H., Hurtmans, D., Pommier, M., Razavi, A., Turquety, S., Wespes, C., and Coheur, P.-F.: Monitoring of atmospheric composition using the thermal infrared IASI/MetOp sounder, *Atmos. Chem. Phys.*, 9, 6041–6054, doi:10.5194/acp-9-6041-2009, 2009.
- Coheur, P.-F., Barret, B., Turquety, S., Hurtmans, D., Hadji-Lazaro, J., and Clerbaux, C.: Retrieval and characterization of ozone vertical profiles from a thermal infrared nadir sounder, *J. Geophys. Res.*, 110, D24303, doi:10.1029/2005JD005845, 2005.
- Crutzen, P. J. and Andreae, M. O.: Biomass burning in the tropics: Impact on atmospheric chemistry and biogeochemical cycles, *Science*, 250, 1669–1678, 1990.
- Dufлот, V., Dils, B., Baray, J.-L., De Mazière, M., Atti, J.-L., Vanhaelewyn, G., Senten, C., Vigouroux, C., Clain, G., and Delmas, R.: Analysis of the origin of the distribution of CO in the subtropical southern Indian Ocean in 2007, *J. Geophys. Res.*, 115, D22106, doi:10.1029/2010JD013994, 2010.
- Gamache, R. R., Lamouroux, J., Laraia, A. L., Hartmann, J.-M., and Boulet, C.: Semiclassical calculations of half-widths and line shifts for transitions in the 30012←00001 and 30013←00001 bands of CO<sub>2</sub>, I: Collisions with N<sub>2</sub>, *J. Quant. Spectrosc. Ra.*, 113, 976–990, 2012.
- Hartmann, J.-M., Boulet, C., and Robert, D.: Collisional Effects on Molecular Spectra, Laboratory Experiments and Models, Consequences for Applications, Elsevier Edition, ISBN: 978-0-444-52017-3, 2008.
- Hurtmans, D., Coheur, P.-F., Wespes, C., Clarisse, L., Scharf, O., Clerbaux, C., Hadji-Lazaro, J., George, M., and Turquety, S.: FORLI radiative transfer and retrieval code for IASI, *J. Quant. Spectrosc. Ra.*, 113, 1391–1408, 2012.
- Lamouroux, J., Gamache, R. R., Laraia, A. L., Hartmann, J.-M., and Boulet, C.: Semiclassical calculations of half-widths and line shifts for transitions in the 30012←00001 and 30013←00001 bands of CO<sub>2</sub> II: Collisions with O<sub>2</sub> and air, *J. Quant. Spectrosc. Ra.*, 113, 991–1003, 2012a.
- Lamouroux, J., Gamache, R. R., Laraia, A. L., Hartmann, J.-M., and Boulet, C.: Semiclassical calculations of half-widths and line shifts for transitions in the 30012←00001 and 30013←00001 bands of CO<sub>2</sub>. III: Self collisions, *J. Quant. Spectrosc. Ra.*, 113, 1536–1546, 2012b.
- Li, Q., Jacob, D., Bey, I., Yantosca, R., Zhao, Y., Kondo, Y., and Notholt, J.: Atmospheric hydrogen cyanide (HCN): Biomass burning source, ocean sink?, *Geophys. Res. Lett.*, 27, 357–360, 2000.
- Li, Q., Palmer, P. I., Pumphrey, H. C., Bernath, P., and Mahieu, E.: What drives the observed variability of HCN in the troposphere and lower stratosphere?, *Atmos. Chem. Phys.*, 9, 8531–8543, doi:10.5194/acp-9-8531-2009, 2009.
- Logan, J. A., Prather, M. J., Wofsy, S. C., and McElroy, M. B.: Tropospheric chemistry: A global perspective, *J. Geophys. Res.*, 86, 7210–7254, 1981.
- Lupu, A., Kaminski, J. W., Neary, L., McConnell, J. C., Toyota, K., Rinsland, C. P., Bernath, P. F., Walker, K. A., Boone, C. D., Nagahama, Y., and Suzuki, K.: Hydrogen cyanide in the upper troposphere: GEM-AQ simulation and comparison with ACE-FTS observations, *Atmos. Chem. Phys.*, 9, 4301–4313, doi:10.5194/acp-9-4301-2009, 2009.
- Mahieu, E., Duchatelet, P., Bernath, P. F., Boone, C. D., De Mazière, M., Demoulin, P., Rinsland, C. P., Servais, C., and Walker, K. A.: Retrievals of C<sub>2</sub>H<sub>2</sub> from high-resolution FTIR solar spectra recorded at the Jungfraujoch station (46.5° N) and comparison with ACE-FTS observations, *Geophys. Res. Abstract*, 10,

- EGU2008-A-00000, 2008.
- Parker, R. J., Remedios, J. J., Moore, D. P., and Kanawade, V. P.: Acetylene C<sub>2</sub>H<sub>2</sub> retrievals from MIPAS data and regions of enhanced upper tropospheric concentrations in August 2003, *Atmos. Chem. Phys.*, 11, 10243–10257, doi:10.5194/acp-11-10243-2011, 2011.
- Pumphrey, H. C., Santee, M. L., Livesey, N. J., Schwartz, M. J., and Read, W. G.: Microwave Limb Sounder observations of biomass-burning products from the Australian bush fires of February 2009, *Atmos. Chem. Phys.*, 11, 6285–6296, doi:10.5194/acp-11-6285-2011, 2011.
- Rodgers, C. D.: Inverse methods for atmospheric sounding: Theory and Practice, Series on Atmospheric, Oceanic and Planetary Physics – Vol. 2, World Scientific Publishing CO., Singapore, 2000.
- Rodgers, C. D. and Connor, B. J.: Intercomparison of remote sounding instruments, *J. Geophys. Res.*, 108, 4116, doi:10.1029/2002JD002299, 2003.
- Rothman, L. S., Gordon, I. E., Barbe, A., Chris Benner, D., Bernath, P. F., Birk, M., Boudon, V., Brown, L. R., Campargue, A., Champion, J.-P., Chance, K., Coudert, L. H., Dana, V., Devi, V. M., Fally, S., Flaud, J.-M., Gamache, R. R., Goldman, A., Jacquemart, D., Kleiner, I., Lacome, N., Lafferty, W. J., Mandin, J.-Y., Massie, S. T., Mikhailenko, S. N., Miller, C. E., Moazzen-Ahmadi, N., Naumenko, O. V., Nikitin, A. V., Orphal, J., Perevalov, V. I., Perrin, A., Predoi-Cross, A., Rinsland, C. P., Rotger, M., Simeckova, M., Smith, M. A. H., Sung, K., Tashkun, S. A., Tennyson, J., Toth, R. A., Vandaele, A. C., and Vander Auwera, J.: The HITRAN 2008 molecular spectroscopic database, *J. Quant. Spectrosc. Ra.*, 110, 533–572, 2009.
- Sinha, P., Hobbs, P. V., Yokelson, R. J., Bertschi, I. T., Blake, D. R., Simpson, I. J., Gao, S., Kirchstetter, T. W., and Novakov, T.: Emissions of trace gases and particles from savanna fires in southern Africa, *J. Geophys. Res.*, 108, 8487, doi:10.1029/2002JD002325, 2003.
- Standard Atmosphere 1976, National Atmospheric and Oceanic Administration S/T 76-1562, US Government Printing Office, Washington D.C., 1976.
- Vigouroux, C., Stavrakou, T., Whaley, C., Dils, B., Dufлот, V., Hermans, C., Kumps, N., Metzger, J.-M., Scolas, F., Vanhaelewyn, G., Müller, J.-F., Jones, D. B. A., Li, Q., and De Mazière, M.: FTIR time-series of biomass burning products (HCN, C<sub>2</sub>H<sub>6</sub>, C<sub>2</sub>H<sub>2</sub>, CH<sub>3</sub>OH, and HCOOH) at Reunion Island (21° S, 55° E) and comparisons with model data, *Atmos. Chem. Phys.*, 12, 10367–10385, doi:10.5194/acp-12-10367-2012, 2012.
- Volkamer, R., Ziemann, P. J., and Molina, M. J.: Secondary Organic Aerosol Formation from Acetylene (C<sub>2</sub>H<sub>2</sub>), seed effect on SOA yields due to organic photochemistry in the aerosol aqueous phase, *Atmos. Chem. Phys.*, 9, 1907–1928, doi:10.5194/acp-9-1907-2009, 2009.
- Wiegele, A., Glatthor, N., Höpfner, M., Grabowski, U., Kellmann, S., Linden, A., Stiller, G., and von Clarmann, T.: Global distributions of C<sub>2</sub>H<sub>6</sub>, C<sub>2</sub>H<sub>2</sub>, HCN, and PAN retrieved from MIPAS reduced spectral resolution measurements, *Atmos. Meas. Tech.*, 5, 723–734, doi:10.5194/amt-5-723-2012, 2012.
- Xiao, Y., Jacob, D. J., and Turquety, S.: Atmospheric acetylene and its relationship with CO as an indicator of air mass age, *J. Geophys. Res.-Atmos.*, 112, D12305, doi:10.1029/2006JD008268, 2007.
- Zander, R., Rinsland, C. P., Ehhalt, D. H., Rudolph, J., and Demoulin, P. H.: Vertical column abundance and seasonal cycle of acetylene, C<sub>2</sub>H<sub>2</sub>, above the Jungfrauoch station, derived from IR solar observations (1991), *J. Atmos. Chem.*, 13, 389–372, 1991.